DOI: 10.61782/fa.2025.0876

FORUM ACUSTICUM EURONOISE 2025

THE OCEANSOUNDMODEL: A GUI FOR SHIPPING NOISE PREDICTIONS

Orlando Camargo Rodríguez **Sérgio Jesus**

Hugues Chognot **Luciano Oliveira Júnior**

LARSys, Universidade do Algarve, Faro 8005-139, Portugal

ABSTRACT

The TRIDENT project is a European initiative, that aims at the development of technological capabilities for the monitoring of deep sea exploration activities. A particular goal of the project is the development of a computational tool for the prediction of acoustic noise levels generated by such activities, that would include also shipping and wind noise. A fundamental support of acoustic predictions is the development of a graphical user interface (GUI), called the OceanSoundModel, that will seamlessly integrate the different types of input data and will also deal with the different time and space scales of the data. While the development of a specific model describing the acoustic noise created by exploration activities is still underway the OceanSoundModel in its current stage is already able to produce noise maps for wind and shipping noise. The discussion presented here describes and showcases the OceanSoundModel, and presents acoustic maps associated with AIS data acquired during the TRIDENT Baseline Survey 2024, that took place near the Tropic Seamount; these maps were able to provide clear guidelines for the identification of quite and noisy ships, as well as revealed important shadow effects of noise levels induced by bathymetric features.

Keywords: *Underwater acoustics, shipping noise, ocean exploration.*

**Corresponding author*: *orodrig@ualg.pt.*

1. INTRODUCTION

The TRIDENT project [1] is an European initiative, that aims at the development of technological capabilities to fully support planning of exploration and production operations related to the extraction of valuable minerals from the seabed, and to provide risk assessments and a complete basis for appropriate operational measures that are protective of marine life and environments, together with guidelines to support policies, regulation and mitigation. While clear standards already exist for the well known (and century-old) oil and gas industry [1,2], deep sea mineral exploration is an area with a fundamental knowledge gap relative to the corresponding impacts that a full-scale industry would have on habitats and environments [3, 4]. The authors, as part of the CINTAL team [2] within the TRIDENT project, are responsible in particular with the task of developing a model for the predictions of acoustic noise as a consequence of deep sea exploration activities; such predictions are to be supported with the development of graphical tools, that will allow the corresponding users to easily combine the different types of input data, while harmonizing the time and space scales of the different inputs. Such tools are integrated under the common name of the ***OceanSoundModel***, a graphical user interface (GUI), that in its current stage is already capable to present acoustic maps combining wind and shipping noise. As an important test of the GUI capabilities AIS shipping data acquired during the TRIDENT Baseline Survey 2024 (TBS'24) was used for the calculation of particular noise maps, providing already clear guidelines for the acoustic classification of ships regarding specific

[1] https://deepseatrident.eu
[2] https://cintal.ualg.pt/

levels of acoustic noise; the maps also revealed important shadow effects on noise levels induced by bathymetric features. The discussion presented here introduces a compact state-of-the-art regarding the general model for predictions of underwater acoustic noise produced by different sources, and a review of the component explicitly related to deep sea exploration activities; the discussion is followed by a description of the OceanSoundModel GUI, presents some of the noise maps calculated for the conditions of the TBS'24 sea trial and proposes further directions of research.

2. STATE OF THE ART

2.1 The general Noise Model

Following the discussion presented in [5] we can write the general model of the acoustic noise level L_m in dB as

$$L_m = 10\log_{10}\left(\sum_{i=1}^{M} N_i\right) \qquad (1)$$

where M is the total number of noise sources and N_i represents the power of the ith source. These powers can differ significantly from one another; therefore, the values of L_m can become dominated in a non-additive way by the largest power.

2.2 Wind Noise

Wind-generated noise can be represented as N_w, defined as

$$N_{wind} = 10^{L_w/10} \qquad (2)$$

where the wind noise level L_w is calculated using the empirical Hildebrand model [6], which (unlike previous models of wind noise) is a model of the acoustic received level; the Hildebrand model was developed using an extensive global dataset of acoustic field recordings, encompassing more than one hundred years of recording-time, with the model explicitly separating noise generated by wind-related sources from noise produced by anthropogenic sources. The recordings captured high wind events and were collected both on shallow continental shelves and in open ocean deep-water settings; code for the model is publicly available [3] .

[3] https://github.com/jahildebrand/WindNoise.

2.3 Shipping Noise

Shipping-generated noise can be represented as $N_{shipping}$, defined as

$$N_{shipping} = \sum_{q=1}^{Q} 10^{(L_s+\mathrm{TL})_q/10} \qquad (3)$$

where Q is the total number of ships and $(L_s)_q$ is the qth ship's sound pressure level (SPL), which is associated with the Automatic Information System (AIS) containing the ship's coordinates, lenght, speed and size. Acoustic disturbances are generated mostly through propeller cavitation noise. The ship's position is coupled with an acoustic propagation model to calculate the transmission loss (TL), with a source depth of 6 m (which on average corresponds to the blades depth); additional knowledge of the local bathymetry, sound speed distribution and acoustic bottom properties is required. The expression L_s+ TL is just the received level RL from the SONAR equation in disguise, where [7]:

$$\mathrm{RL = SL - PL} \qquad (4)$$

with L_s instead of the source level SL and TL as the opposite of propagation loss PL. Among available models it was decided to adopt the recent JOMOPANS-ECHO model [8] for the calculation of L_s; the model relies on a large database of cooperative ships and its code is also publicly available [4] .

2.4 Noise from exploration activities

The research related to the noise power associated with exploration activities can be started with the reference to the ABYSOUND project [9], which was designed to establish services and systems to estimate the noise radiated into the water by equipment deployed on the ground during deep offshore sea floor operations; such study would make possible to assess the acoustic environmental impact on marine fauna, as well as assessing acoustic disturbances on the operation of gliders and remotely operated vehicles. While exploration architectures can vary from one proposal to another ABYSOUND identified four common subsystems of exploration equipment (see Fig. 1), namely:

[4] https://www.mdpi.com/article/10.3390/jmse9040369/s1.

[6] http://www.nautilusminerals.com/irm/content/technology-overview.aspx?RID=329

1. The (bottom located) Seafloor Production Tool (SPT), with noise generated by the propulsion system with the collector equipment moving over the seafloor, crushing of nodules on the ground, and multi-beam echosounder pinging at regular intervals.

2. The (bottom located) Subsea Slurry Lift Pump (SSLP), with noise generated by pumps and hydraulic jets lifting nodules off and cleaning sediments.

3. The (watercolumn) Riser And Lifting System (RALS), with pumps continuously operating to uplift ore to the surface.

4. The (near surface) Production Support Vessel (PSV). Acoustic disturbances generated by the PSV could be generated from different sources, namely thruster cavitation noise (while on location), noise transmitted from the hull to the water due to on board power generators, engines, machinery, vessel activities, ore landing, water cleaning, etc., and even from hull mounted multi-beam echosounders.

Not included here (but possibly a part of the system) are autonomous gliders and remotely operated vehicles, which due to the corresponding sizes can be expected to operate in a relatively silent regime. The discussion presented in [9] concludes that the higher noise levels could be expected to originate from the machinery placed on the ground, and proposes a model with noise spectra from different subsystems exhibiting a constant value between 130 and 170 dB for frequencies from 10 to 100 Hz, followed by a linear decrease of 20 dB per decade (see Fig. 2). Missing in the discussion is the potential coupling of RALS generated noise with the SOFAR channel. A discussion coupled with the calculation of noise maps for the Clarion-Clipperton Zone (CCZ) is presented in [3]. Considered spectra (shown in Fig. 3) were obtained considering the operation in shallow waters of analogs, like coastal dredges that remove seafloor gravel and sediment, pump-out operations from coastal dredging, and floating production storage and offloading (FPSO) vessels used by the oil and gas industry. TL predictions were obtained with 2D models, running along different transects (i.e., out-of-plane propagation was not considered). The TRIDENT related discussion from [10] considered an alternative model, with spectra limited in frequency (see Fig. 4); in this model the bottom located and mid-watercolumn equipment all exhibit a constant level, while the near surface source shows a non-continuous level, with a steady linear decrease. Corresponding excess noise calculations presented in [10] for a seamount and a Munk-like sound speed profile provided predictions of depth-dependent circular zones, separated by sudden changes in noise levels.

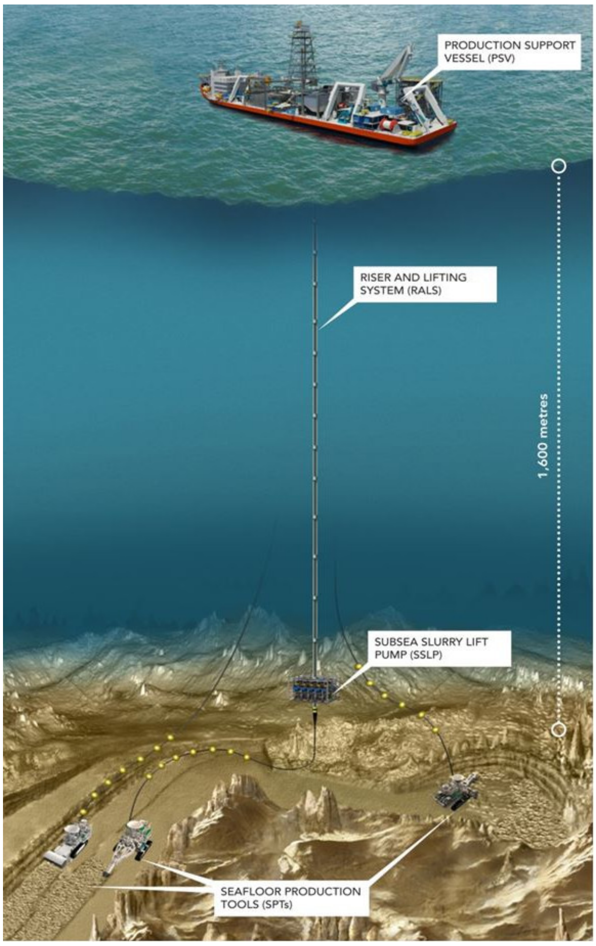

Figure 1. Idealized subsystems of deep sea exploration equipment[6].

3. THE OCEANSOUNDMODEL GUI

The current version of OceanSoundModel (giving the current lack of clear guidelines regarding the acoustic noise generated by exploration activities) implements Eqn. (1) for wind and shipping noise, which allows to rewrite

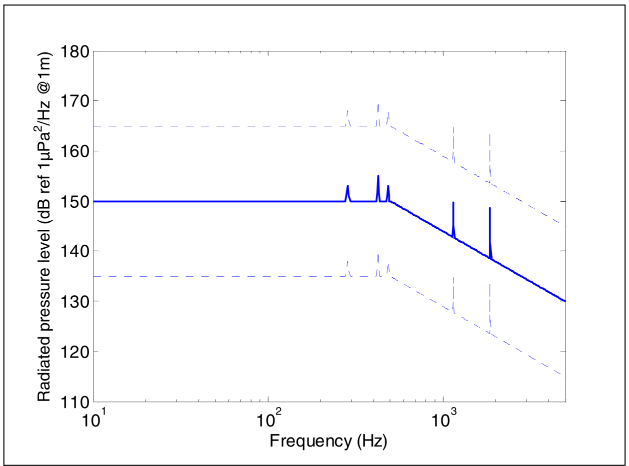

Figure 2. Proposed spectra of radiated noise level (dB ref 1 μPa^2/Hz) at 1 m of the production tools on the ocean floor as a function of frequency (from [**?**]).

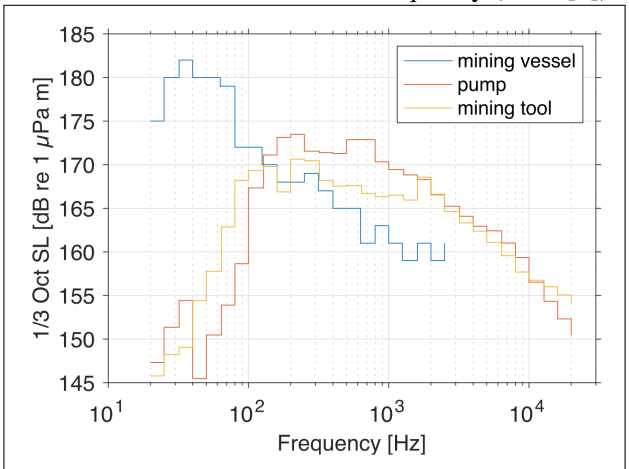

Figure 3. One-third octave source spectra considered in [3]. Monopole source depths are 10 m from the sea surface, every 1 km from the sea surface for the pumps, and 1 m above the seafloor for the bottom located machinery.

Eqn. (1) as

$$L_m = 10 \log_{10} \left(N_{wind} + N_{shipping} \right) \tag{5}$$

As shown in Fig. 5 the GUI has three components , namely:

1. The **Input** component, which defines environmental data, more specifically: bathymetry (from the GEBCO database[5] or from user defined data), wind/temperature/salinity (from the Copernicus online prediction system[6] or from user defined data), ship AIS information and acoustic model parameters (both user defined). Temperature and salinity are converted to sound speed distributions using Mackenzie's formula [11].

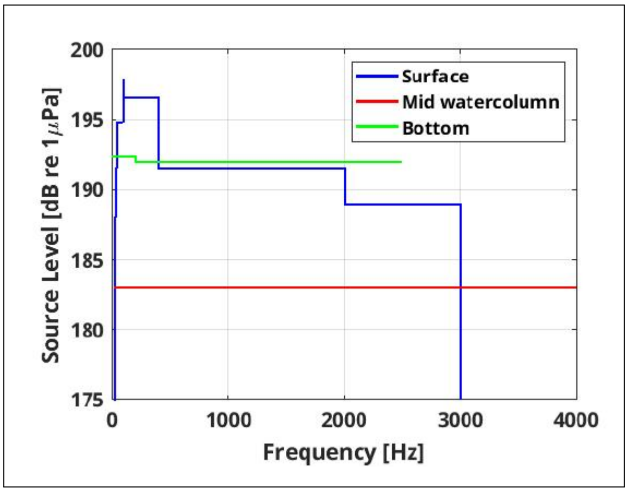

Figure 4. Proposed source level spectrum as a acoustic power sum for three depths: bottom, mid-water and surface (from [10]).

2. The **Model** component, for preliminary visualization of wind noise (using the Hildebrand model), ships SPL (using the JOMOPANS-ECHO model) and ocean exploration activities SPL (currently under development).

3. The **Noise** component, which combines the different inputs for the calculation of noise maps, either considering isolated components of noise powers or considering different combinations.

The GUI can load Matlab user defined *.mat files, as well as GEBCO bathymetry files and Copernicus environmental predictions for the desired time interval. The current version requires pre-processing of AIS data and of acoustic predictions calculated with an underwater 3D model and produces noise maps on a local system of Cartesian coordinates, whose origin and dimensions can be specified by the user. The GUI is carefully coded to prevent

[5] https://www.gebco.net.
[6] https://marine.copernicus.eu.

user input with non-overlapping data.

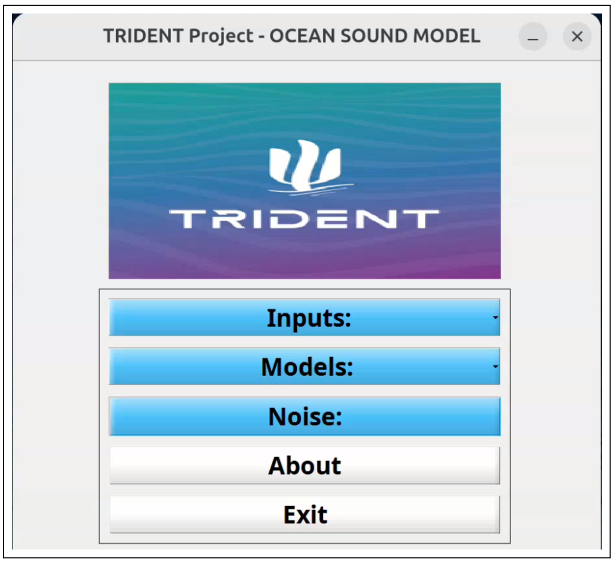

Figure 5. General aspect of the OceanSoundModel GUI, with the set of components for user input, model verification and noise maps output.

Calculations of TL are obtained with the Bellhop3D ray-tracing/Gaussian-beam underwater acoustic model [12], which can include space distributions of sound speed, and can generate cylindrical predictions with a given radius, centered at the source position, along a desired set of receiver depths. Before GUI integration Bellhop3D's results were compared with predictions from other models considering idealized scenarios, without detecting significant divergences between the results. To implement the calculation of transmission loss in (3) within the OceanSoundModel all geographical coordinates are converted into local Cartesian coordinates, and each grid of transmission loss, centered at a ship's position, needs to be re-interpolated on the local grid. Source aperture $2\theta_{max}$ is considered to be constant, and given by the expression

$$\theta_{max} = \arccos\left(\frac{c_w}{c_b}\right) \tag{6}$$

where $c_w = \min c$, c stands for the sound speed in the watercolumn and c_b represents the compressional bottom sound speed. If desired the user can let Bellhop3D choose the number of rays; however, it was decided to rely on the relationship $N_{rays} = 2N_{modes}$, where the number of modes is given by the empirical expression [13]

$$N_{modes} = \frac{2Df}{c_w}\frac{\ln\left(\sqrt{1-c_w/c_b}+1\right)}{\ln 2} + 1/2 \tag{7}$$

with D representing bottom depth at the source position. The higher the frequency f the larger N_{rays} becomes, drastically increasing calculation times near and after the kHz range.

3.1 The TBS'24

The area chosen for TRIDENT system demonstration was the Tropic Seamount (TS), located to the south of Canary Islands (see Fig. 6), which is well known for its deposits of polymetallic nodules; the large scale bathymetry around it is defined by a slight sloping bottom in the EW direction with 500 m depth increment per 100 km. The TS rises from approximately 4000 m to 1000 m depth at its shallowest and has a shape that resembles a 4-pointed star, aligned with the cardinal directions. The bottom at the summit is relatively smooth with a maximum bathymetry difference of 50 m in its center. Support for research activities was provied by the IPMA research vessel *Mário Ruivo*,with CINTAL and ALSEAMAR in charge of glider deployment and navigation, as well as collecting AIS data for noise predictions. The TBS'24 took place from 13th June to 2nd July 2024.

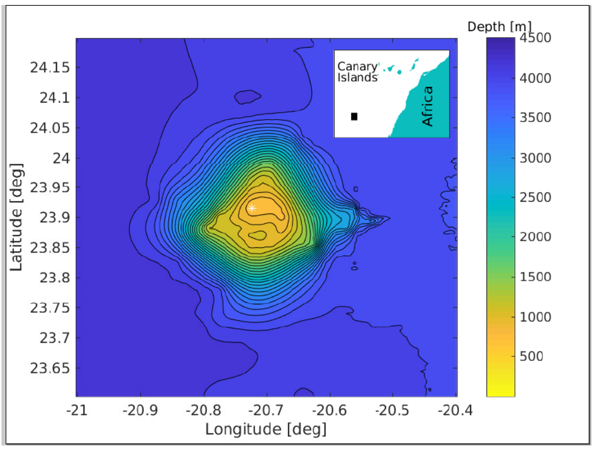

Figure 6. Bathymetry of the Tropic Seamount.

4. PRELIMINARY SOUND MAPS

A partial set of noise maps was calculated with the OceanSoundModel GUI on a local cartesian grid of

400km×400km, with the TS as the origin, for a frequency of 63 Hz and a depth of 100 m, over a period of 6 hours, starting at 00:00 of June 20 2024. Bellhop3D can account for a variable distribution of bottom types in a given area, but for simplicity the bottom was considered to be uniform, composed mostly by sand, with bottom properties given by the set of parameters shown in Tab. 1.

Table 1. Acoustic bottom properties.

Property	Symbol	Value	Units
Compress. sound speed	c_b	1750	m/s
Shear sound speed	c_s	0	m/s
Compress. attenuation	α_b	0	dB/λ
Shear attenuation	α_s	0	dB/λ
Density	ρ	2	g/cm^3

Wind, salinity and temperature predictions were calculated with the Copernicus Marine Toolbox for the corresponding time interval; sound speed distributions were calculated from temperature and salinity accordingly; careful analysis of those distributions revealed very little variability over time and on the horizontal plane; therefore, the acoustic model used an average of the space anf time distributions (which was found to resemble a Munk profile). Some of the results are shown in Fig. 7, Fig. 8 and Fig. 9. For a better understanding of different features each case shows the ships positions, the corresponding SPLs calculated with the JOMOPANS-ECHO model, and bathymetry contours to visualize the ships positions relative to the TS; the color convention uses gray tones, in which, the darker the icon the higher the SPL. Timestamps are placed on top of each noise map for proper reference, and the background color distribution reflects the space (and time variability) of wind noise at every instant. The maps perfectly show that the ships can be grouped according to the following categories:

1. “Quiet” ships, with an SPL below 140 dB; they produce a noise that blends with wind noise, as shown in Fig. 7.
2. “Average” ships, with an SPL between 140 and 150 dB; these ships produce a noise slightly above wind noise, as shown in Fig. 8.
3. “Noisy” ships, with an SPL above 150 dB; such ships produce a noise that dominates the noise map, as shown in Fig. 9.

Besides the ships “noiseness” the presence of the TS played an important role in the noise distribution by partially blocking the noise field, creating areas where noise intensity can drop significantly, as shown in Fig. 9.

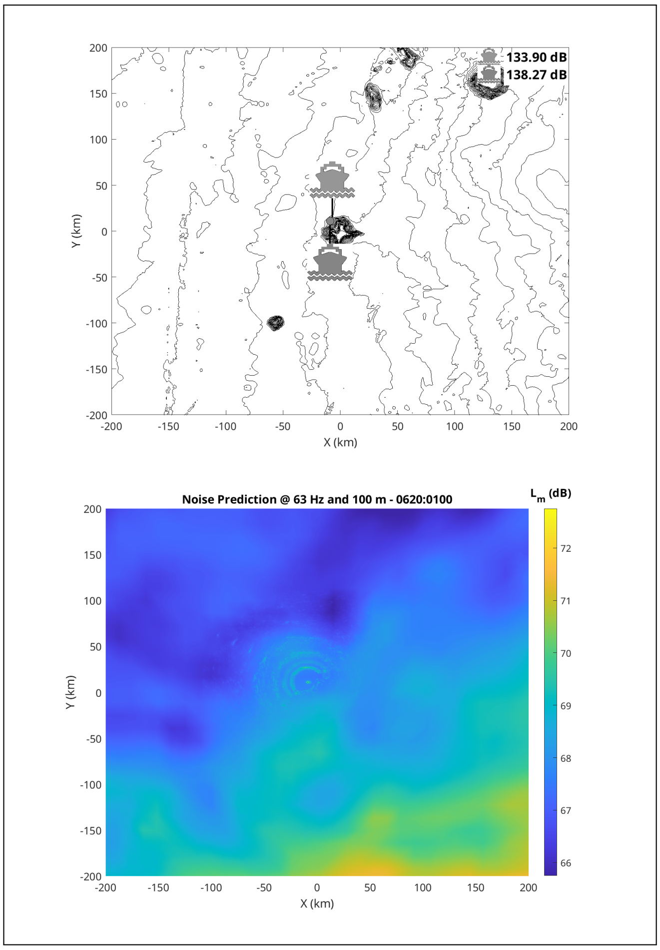

Figure 7. “Quiet” ships positions, with corresponding SPLs (top) and corresponding noise map (bottom).

5. CONCLUSIONS

Noise maps calculated with the OceanSoundModel provided an insightful reference regarding noise levels from shipping traffic, revealing shadow effects induced by the bathymetry and a potential classification of ships relative to the corresponding SPLs. Still, the development of the

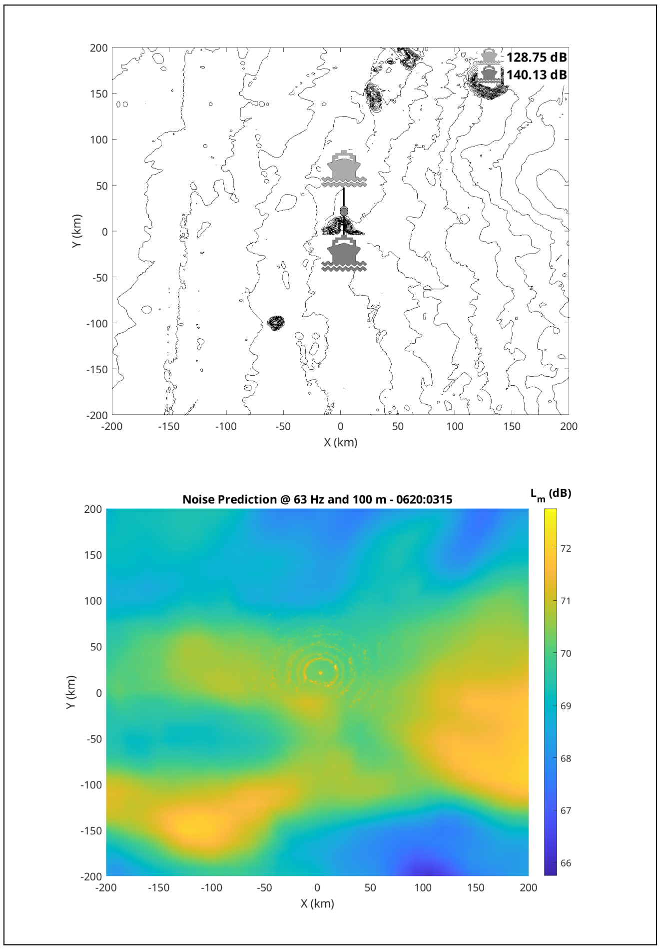

Figure 8. “Average” ships positions, with corresponding SPLs (top) and corresponding noise map (bottom).

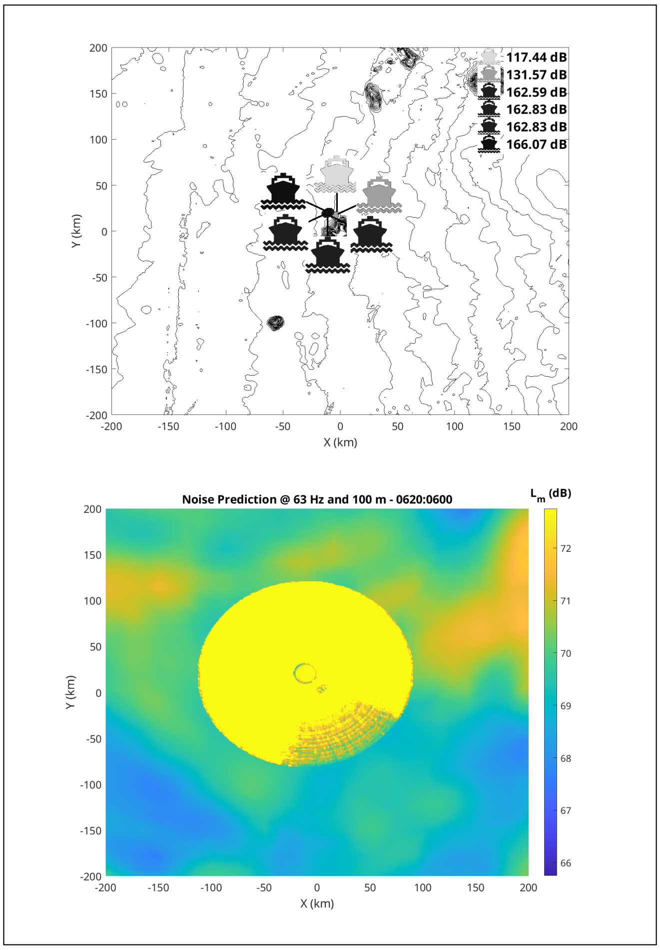

Figure 9. “Noisy” ships positions, with corresponding SPLs (top) and corresponding noise map (bottom); the shadowing effect of the Tropic Seamount is evident.

GUI must continue in order to address important issues, namely:

- Speeding up of acoustic model predictions near and beyond the kHz range, which currently can take several hours.
- Removal of numerical artifacts induced by the placement of acoustic sources on nodes of the bathymetry when working with space distributions of sound speed.
- Development of an acoustic noise model for exploration activities, which can be easily integrated into the final version of the GUI.
- GUI extension to allow:
  - raw-input of AIS data and direct running of the acoustic model for desired frequencies;
  - calculation of excess noise levels;
  - running as an online web service.
- Extensive validation and calibration of predictions.
- Preparation of documentation and reference examples.
- Design of a modular architecture, which will allow the integration of the OceanSoundModel with tools

to include the distribution of marine species and the calculation of risk maps.

Further research into the topic will continue with the development of a second TRIDENT campaign in 2025.

6. ACKNOWLEDGMENTS

This work was performed under the TRIDENT project, that has received funding from the European Union's HE programme under grant agreement No 101091959.

7. REFERENCES

[1] C. de Jong et al., "Measurement procedures for underwater sound sources associated with oil and gas exploration and production activities.," Tech. Rep. 4, TNO, 2021.

[2] M. A. Ainslie, P. H. Dahl, C. A. F. de Jong, and R. M. Laws, "Practical spreading laws: The snakes and ladders of shallow water acoustics," in *Proc. of UA2014*, (Rhodes, Greece), pp. 879–886, 2014.

[3] R. Williams, C. Erbe, A. Duncan, K. Nielsen, T. Washburn, and C. Smith, "Noise from deep-sea mining is likely to ensonify large areas of the ocean," *Science*, vol. 377, no. 6602, pp. 157–158, 2022.

[4] C. Martin, L. Weilgart, D. J. Amon, and J. Müller, "Deep-Sea Mining: A noisy affair," tech. rep., Ocean Care, 2021.

[5] S. M. M. Jesus, C. Soares, M. Romagosa, I. Cascão, R. Duarte, F. Zabel, and M. SILVA, "A Methodology for Shipping Noise Field Calibration and Excess Noise Estimation: the Azores Case Study," *J. Mar. Sci. Eng. (JMSE)*, no. 10, pp. 1763–1778, 2022.

[6] J. A. Hildebrand, K. Frasier, S. Baumann-Pickering, and S. Wiggins, "An empirical model for wind-generated ocean noise," *J. Acoust. Soc. America*, no. 149, pp. 4516–4533, 2021.

[7] O. C. Rodríguez, *Fundamentals of Underwater Acoustics*. Springer Nature Switzerland AG 2023: Springer, 2023.

[8] A. MacGillivray and C. de Jong, "A reference spectrum model for estimating source levels of marine shipping based on automated identification system data," *Journal of Marine Science and Engineering*, vol. 9, no. 4, pp. 369–374, 2021.

[9] R. Bassila, T. Bertet, L. Somaglino, M.-E. Bouhier, H. Glotin, and P. Best, "Abysound, an end to end system for noise impact measurement of deep sea mining production tools," in *Proc. of OCEANS 2019*, (Marseille, France), pp. 1–9, 2019.

[10] S. M. M. Jesus and O. C. Rodríguez, "Estimating excess noise from deep sea mining: a simulated test case," in *Proc. of OCEANS 2023*, (Limerick, Ireland), pp. 1–6, 2023.

[11] K. Mackenzie, "Nine-term equation for the sound speed in the oceans," *J. Acoust. Soc. America*, vol. 70, no. 3, pp. 807–812, 1981.

[12] M. B. Porter, "BELLHOP3D User Guide," tech. rep., HLS, 2015.

[13] F. Jens and M. Ferla, "SNAP: The SACLANTCEN normal-mode acoustic propagation model," Tech. Rep. 121, SACLANTCEN, April 1979.